Inorganic Chemistry

Article

pubs.acs.org/IC

Syntheses, Crystal Structures, Transport Properties, and Theoretical Studies of Five Members of the MAn_2Q_5 Family: SrU_2S_5, BaU_2Se_5, PbU_2S_5, $BaTh_2S_5$, and BaU_2Te_5

Jai Prakash,[†] Mariya S. Tarasenko,[†] Adel Mesbah,[†,‡] Sébastien Lebègue,[§] Christos D. Malliakas,[†] and James A. Ibers*[,†]

[†]Department of Chemistry, Northwestern University, 2145 Sheridan Road, Evanston, Illinois 60208-3113, United States

[‡]ICSM, UMR 5257 CEA/CNRS/UM2/ENSCM, Site de Marcoule - Bât. 426, BP 17171, 30207 Bagnols-sur-Cèze cedex, France

[§]Laboratoire de Cristallographie, Résonance Magnétique et Modélisations (CRM2, UMR CNRS 7036), Institut Jean Barriol, Université de Lorraine, BP 239, Boulevard des Aiguillettes, 54506 Vandoeuvre-lès-Nancy, France

Supporting Information

ABSTRACT: Five compounds of the MAn_2Q_5 family, namely, SrU_2S_5, BaU_2Se_5, PbU_2S_5, $BaTh_2S_5$, and BaU_2Te_5, have been synthesized by high-temperature solid-state reactions. The crystal structures of these compounds were determined by single-crystal X-ray diffraction studies. SrU_2S_5, BaU_2Se_5, PbU_2S_5, and $BaTh_2S_5$ crystallize in the PbU_2Se_5 structure type in space group C_{2h}^5–$P2_1/c$ of the monoclinic system, whereas BaU_2Te_5 adopts the $(NH_4)Pb_2Br_5$ structure type in space group D_{4h}^{18}–$I4/mcm$ of the tetragonal system. There are no Q–Q bonds in these structures, so the formulas charge balance as $M^{2+}(An^{4+})_2(Q^{2-})_5$. The An atoms in the monoclinic structure are seven- or eight-coordinated by Q atoms; the U atoms in the tetragonal structure are eight-coordinated. The M atoms in the monoclinic structure are coordinated to either eight or nine Q atoms, depending on the monoclinic β angle; the M atoms in the tetragonal structure are 10-coordinated. Resistivity studies on single crystals of SrU_2S_5, BaU_2Se_5, and PbU_2S_5 show metallic behavior with resistivities of 0.24, 10, and 3.3 mΩ·cm, respectively, at 298 K. Spin-polarized density functional theory in the generalized gradient approximation applied to the four U compounds suggests that they are ferromagnetic. In each compound, the density of states of one spin channel is found to be finite at the Fermi level, whereas there is a gap in the density of states of the other spin channel; this is characteristic of a half-metal.

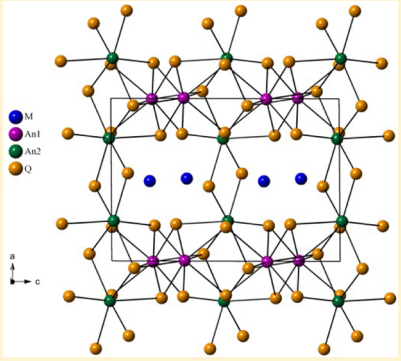

INTRODUCTION

The study of actinide-based materials has important implications in the nuclear fuel cycle. For example, there is increased interest in the use of metal chalcogenides for selective removal of nonactinide fission products,[1−4] such as alkaline-earth metals, in particular ^{90}Sr.[4] A variety of actinide chalcogenides, An/Q (An = U, Th, or Np; Q = S, Se, or Te), are known,[5−7] and many exhibit interesting physical properties (magnetic, electronic, or optical) engendered by the f-electrons of actinides.[5−10] The known ternary compounds Ak/An/Q (Ak = alkaline-earth metal) include Ba_2AnS_6 (An = U, Th),[9] $BaUS_3$,[11−13] $AkUS_2$ (Ak = Ca and Sr),[14] and $AkAn_2Q_5$ (Ak = Ca, Sr, Ba, or Pb; An = U, Th).[10,15−17] The structures of the compounds AkU_2S_5 (Ak = Ca, Sr, Ba),[15] on the basis of X-ray powder diffraction studies, and the compounds MU_2S_5 (M = Pb, Eu) and MU_2Se_5 (M = Ca, Sr, Ba, Pb, and Eu), on the basis of single-crystal X-ray diffraction data, were originally described in the orthorhombic system,[16] somewhat analogous to the structures of U_3S_5[18] and U_3Se_5.[19] However, later studies found that PbU_2Se_5,[17] $SrTh_2Se_5$,[10] and BaU_2S_5[13] crystallize in the monoclinic system.

In this paper, we present the syntheses, crystal structures, and transport and electronic properties of five members of the MAn_2Q_5 family, namely, SrU_2S_5, BaU_2Se_5, PbU_2S_5, BaU_2Te_5, and $BaTh_2S_5$. The sulfide and selenide compounds crystallize in the monoclinic system in the PbU_2Se_5 structure type, whereas BaU_2Te_5 crystallizes in the tetragonal system in the $(NH_4)Pb_2Br_5$ structure type. Transport measurements performed on the uranium sulfides and selenides have shown a metallic behavior with resistivity values of 0.24, 3.3, and 10 mΩ·cm for SrU_2S_5, PbU_2S_5, and BaU_2Se_5, respectively. These results are consistent with those from DFT calculations using the GGA functional.

EXPERIMENTAL METHODS

Syntheses. The following reactants were used as obtained: SrS (Alfa, 99.9%), Ba (Johnson Matthey, 99.5%), Th (MP Biomedicals, 99.1%), S (Mallinckrodt, 99.6%), Se (Cerac, 99.999%), Te (Aldrich, 99.8%), Sb_2S_3 (Alpha, 99%), Pb (Aldrich, 99.95%), and CsCl (Aldrich, 99.9%). Depleted U powder was obtained by hydridization and

Received: July 24, 2014
Published: October 10, 2014

   dx.doi.org/10.1021/ic501795w | Inorg. Chem. 2014, 53, 11626−11632

Table 1. Crystallographic Data and Structure Refinement Details for Five Members of the MAn_2Q_5 Family[a]

	SrU_2S_5	BaU_2Se_5	PbU_2S_5	$BaTh_2S_5$	BaU_2Te_5
space group	C_{2h}^5–$P2_1/c$	C_{2h}^5–$P2_1/c$	C_{2h}^5–$P2_1/c$	C_{2h}^5–$P2_1/c$	D_{4h}^{18}–$I4/mcm$
a (Å)	8.2700(17)	8.7606(1)	8.2376(4)	8.6100(17)	8.3194(2)
b (Å)	7.4400(15)	7.8316(1)	7.4434(3)	7.6200(15)	8.3194(2)
c (Å)	11.720(2)	12.2399(2)	11.7236(5)	12.060(2)	14.5620(4)
β (deg)	90.40(3)	90.527(1)	90.139(2)	90.34(3)	
V (Å^3)	721.1(2)	839.74(2)	718.84(5)	791.2(3)	1007.87(6)
ρ (g cm^{-3})	6.669	7.975	7.795	6.395	8.247
μ (mm^{-1})	53.507	64.687	69.646	43.634	50.026
$R(F)^b$	0.023	0.026	0.040	0.037	0.017
$R_w(F_o^2)^c$	0.054	0.063	0.117	0.064	0.041

[a]For all structures, λ = 0.71073 Å, T = 100(2) K, Z = 4. [b]$R(F) = \sum||F_o| - |F_c||/\sum|F_o|$, for $F_o^2 > 2\sigma(F_o^2)$. [c]$R_w(F_o^2) = \{\sum[w(F_o^2 - F_c^2)^2]/\sum wF_o^4\}^{1/2}$. For $F_o^2 < 0$, $w^{-1} = \sigma^2(F_o^2)$; for $F_o^2 \geq 0$, $w^{-1} = \sigma^2(F_o^2) + (qF_o^2)^2$, where q = 0.0056 for SrU_2S_5, 0.0204 for BaU_2Se_5, 0.0490 for PbU_2S_5, 0.0153 for $BaTh_2S_5$, and 0.0065 for BaU_2Te_5.

decomposition of turnings (IBI Labs) in a modification[20] of a previous literature method.[21]

Reactions were performed in sealed 6 mm carbon-coated fused-silica tubes. Chemical manipulations were performed inside an Ar-filled drybox. The reactants were weighed and transferred into tubes that were then evacuated to 10^{-4} Torr, flame-sealed, and placed in a computer-controlled furnace.

Semiquantitative EDX analysis of the products of the reactions were obtained with the use of a Hitachi S-3400 SEM microscope.

Synthesis of SrU_2S_5. Crystals of SrU_2S_5 were obtained from the reaction of SrS (11.2 mg, 0.094 mmol), U (40 mg, 0.168 mmol), S (15 mg, 0.468 mmol), and Sb_2S_3 (66.2 mg, 0.195 mmol) as a flux. The reaction mixture was heated to1223 K in 48 h and annealed for 169 h. The reaction mixture was cooled to 623 K at 5 K/h, and then to 298 K in 60 h. The reaction product contained black block-shaped crystals of SrU_2S_5 (Sr:U:S ≈ 1:2:5), black columnar crystals of Sb_2S_3, black needles of $Sr_3Sb_4S_9$,[22] and black plates of UOS.[23]

Synthesis of BaU_2Se_5. Crystals of BaU_2Se_5 were obtained by the reaction of Ba (5.85 mg, 0.0425 mmol), U (20 mg, 0.084 mmol), Se (16.6 mg, 0.21 mmol), and 200 mg of CsCl as a flux. The reaction mixture was heated to 773 K in 12 h and held there for 12 h. The temperature was then raised to 1173 K in 24 h, where it remained for 96 h. The reaction mixture was then cooled to 973 K in 24 h, and to 298 K in 12 h. The reaction product contained block-shaped crystals of BaSe, unreacted CsCl flux, UOSe, and black plates of BaU_2Se_5 (Ba:U:Se ≈ 1:2:5).

Synthesis of PbU_2S_5. Crystals of PbU_2S_5 were obtained from the reaction of Pb (100 mg, 0.482 mmol), U (20 mg, 0.084 mmol), and S (11 mg, 0.343 mmol). The reaction mixture was heated to 773 K in 12 h, held there for 12 h, and then heated to 1273 K in 24 h, where it remained for 72 h. The reaction mixture was cooled to 1023 K in 48 h and to 298 K in 12 h. The reaction product contained black blocks of PbU_2S_5 (Pb:U:S ≈ 1:2:5), PbS, and black plates of UOS.

Synthesis of $BaTh_2S_5$. Crystals of $BaTh_2S_5$ were obtained from the reaction of Ba (11.8 mg, 0.086 mmol), Th (40 mg, 0.172 mmol), and S (27.6 mg, 0.861 mmol). The reaction mixture was heated to 1073 K in 36 h and then to 1123 K, where it remained for 99 h. It was cooled to 873 K at 2.5 K/h and then to 298 K at 5 K/h. The reaction product contained grayish black crystals of $BaTh_2S_5$ (Ba:Th:S ≈ 1:2:5), BaS, and yellow plates of ThOS.[24]

Synthesis of BaU_2Te_5. This telluride was obtained by the reaction of Ba (5.8 mg, 0.042 mmol), U (20.2 mg, 0.084 mmol), and Te (26.7 mg, 0.21 mmol) in a CsCl (300 mg) flux. The reaction mixture was heated to 773 K in 12 h and kept there for 12 h, and then the temperature was raised to 1173 K in 24 h and held there for 72 h. The reaction mixture was cooled to 673 K in 48 h, and then to 293 K in 12 h. The black thin plates in the reaction product showed Ba:U:Te ≈ 1:2:5. The major product contained Cs, U, Te, and O.

Structure Determinations. The crystal structures of all five compounds were determined from single-crystal X-ray diffraction data collected with the use of graphite-monochromatized MoKα radiation (λ = 0.71073 Å) at 100(2) K on a Bruker APEX2 diffractometer.[25] The algorithm COSMO implemented in the program APEX2 was used to establish the data collection strategy with a series of 0.3° scans in ω and φ. The exposure time was 10 s/frame, and the crystal-to-detector distance was 60 mm. The collection of intensity data as well as cell refinement and data reduction was carried out with the use of the program APEX2.[25] Face-indexed absorption, incident beam, and decay corrections were performed with the use of the program SADABS.[26] Precession images of the data sets provided no evidence for supercells. All structures were solved and refined in a straightforward manner with the use of the Shelx-14 algorithms of the SHELXT program package.[26,27] The program STRUCTURE TIDY[28] in PLATON[29] was used to standardize the atomic positions. Further details are given in Table 1 and in the Supporting Information.

Resistivity Studies. Four-probe temperature-dependent resistivity data were collected using a homemade resistivity apparatus equipped with a Keithley 2182 nanovoltmeter, a Keithley 236 source measure unit, and a high-temperature vacuum chamber controlled by a K-20 MMR system. An I–V curve from 1×10^{-5} to -1×10^{-5} A with a step of 2×10^{-6} A was measured for each temperature point, and resistance was calculated from the slope of the I–V plot. Data acquisition was controlled by custom-written software. Graphite paint (PELCO isopropanol-based graphite paint) was used for electrical contacts with Cu of 0.025 mm in thickness (Omega). Direct current was applied along an arbitrary direction.

Theoretical Calculations. The Vienna Ab initio Simulation Package[30,31] in the framework of the projector augmented wave method[32] was used to perform the ab initio calculations. In this procedure, the wave functions are expanded as a combination of plane waves with localized orbitals, leading to a very efficient and robust scheme. Spin-polarized density functional theory[33,34] in the generalized gradient approximation[35] was used to obtain the electronic structures. The crystal geometries used in our calculations were fixed at the experimental structures, and the various possible magnetic orders that can occur in a single unit cell were computed in order to compare their total energies, the ground state magnetic configuration being the one with the lowest energy. To obtain convergence, we have used the default cutoff for the wave functions and a k-point mesh of 4 × 4 × 3 to sample the Brillouin zone.

RESULTS AND DISCUSSION

Syntheses. Single crystals of the compounds SrU_2S_5, BaU_2Se_5, PbU_2S_5, $BaTh_2S_5$, and BaU_2Te_5 were obtained in yields of about 50, 90, 50, 20, and 10 wt %, respectively. No attempt was made to maximize these yields.

As noted above, each of these compounds was contaminated by other phases, most commonly by the very stable actinide oxychalcogenide. Oxygen contamination prevades high-temperature solid-state reactions involving the highly oxyphilic actinides.[36] In this instance, such contamination has made it

dx.doi.org/10.1021/ic501795w | Inorg. Chem. 2014, 53, 11626–11632

impossible to determine magnetic properties, although an attempt was made for BaU_2Se_5, for which single crystals were obtained in the highest yield. After manual removal of the white crystals of excess CsCl flux and the large crystals of BaSe, the remaining reaction product was ground. An X-ray powder diffraction pattern showed BaU_2Se_5 to be the major phase but UOSe to be the minor phase. A magnetic measurement from 298 to 5 K on this powdered sample showed an antiferromagnetic transition around 75 K where the transition in UOSe occurs.[37,38] Thus, BaU_2Se_5 shows no magnetic transition down to 5 K and is paramagnetic. Unfortunately, the presence of UOSe in the sample did not allow the determination of the magnetic properties of BaU_2Se_5.

Crystal Structures. The compounds SrU_2S_5, BaU_2Se_5, PbU_2S_5, and $BaTh_2S_5$ crystallize in the PbU_2Se_5[17] structure type with four formula units in space group C_{2h}^5–$P2_1/c$ of the monoclinic system. In contrast, the compound BaU_2Te_5 crystallizes in the $(NH_4)Pb_2Br_5$[39] structure type with four formula units in space group D_{4h}^{18}–$I4/mcm$ of the tetragonal system. Crystallographic details on these five structures are given in Table 1 and in the Supporting Information.

SrU_2S_5, BaU_2Se_5, PbU_2S_5, and $BaTh_2S_5$. Figure 1 shows a general view of the unit cell of these isostructural compounds of

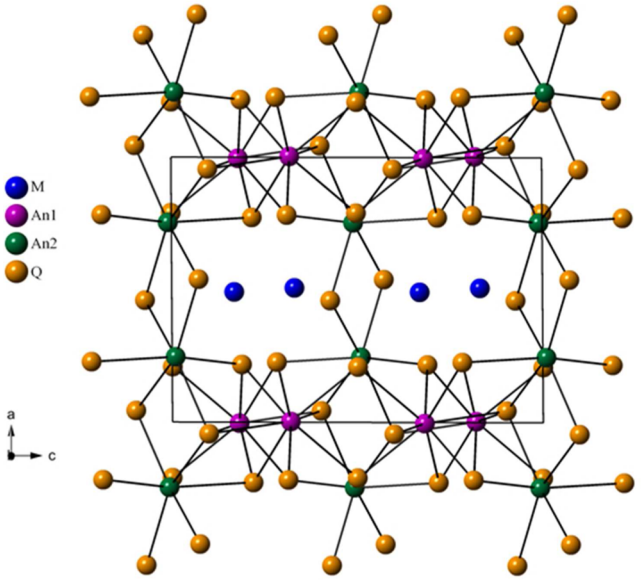

Figure 1. Crystal structure of the isostructural MAn_2Q_5 compounds SrU_2S_5, BaU_2Se_5, PbU_2S_5, and $BaTh_2S_5$.

the MAn_2Q_5 family. The asymmetric unit of these structures comprises two crystallographically unique An atoms, one M atom, and five Q atoms, all in general positions. Each An1 atom is surrounded by eight Q atoms to form a bicapped trigonal prism, whereas the An2 atoms are coordinated to seven Q atoms in a distorted face-capped octahedron. The An1 network is formed by sharing of edges of the trigonal prism face with three An1 neighbors, two of which share caps as well (Figure 2). The An2 atoms are edge-shared along the *a* axis (Figure 3). Finally, the channels oriented along the [010] direction are filled by M atoms that are coordinated to eight or nine Q atoms depending on M (Figure 4). Note that when the β angle in these compounds is closer to 90°, as in PbU_2Se_5 (90°),[17] $SrTh_2Se_5$ (90.00(2)°),[10] and PbU_2S_5 (90.139(2)°), then the coordination number of M is eight (Figure 4a), and the

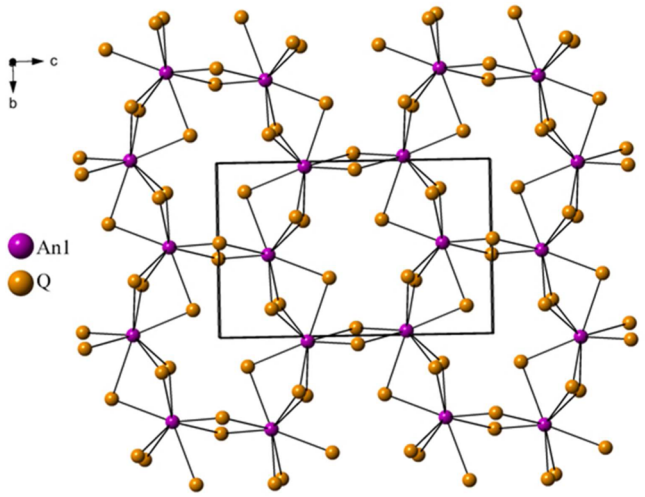

Figure 2. An1 network viewed along the [100] direction in the isostructural MAn_2Q_5 compounds SrU_2S_5, BaU_2Se_5, PbU_2S_5, and $BaTh_2S_5$.

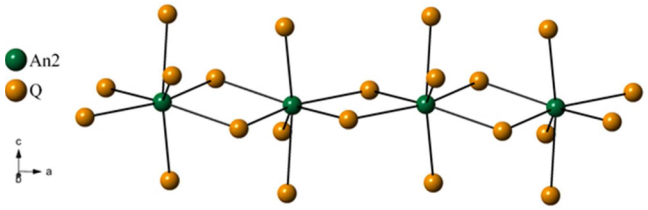

Figure 3. Infinite An2 chain viewed along approximately the [010] direction in the isostructural MAn_2Q_5 compounds SrU_2S_5, BaU_2Se_5, PbU_2S_5, and $BaTh_2S_5$.

coordination geometry is similar to that of the An1 atom. Deviation of the β angle from 90° leads to an increase in the coordination number of M from eight to nine in $BaTh_2S_5$ (90.34(3)°), SrU_2S_5 (90.40(3)°), BaU_2Se_5 (90.527(1)°), and BaU_2S_5 (90.613(2)°) (Figure 4b).[13]

As a result of the eight coordination of the An1 atom versus the seven coordination of the An2 atom, the An1–Q interatomic distances are consistently longer than the corresponding An2–Q distances (Table 2). The U–S distances in the MU_2S_5 structures are consistent with those observed in the structures of Ba_2US_6 (2.734 (2)–2.820(1) Å)[9] and $BaUS_3$ (2.668(1)–2.696(1) Å).[13] The U–Se distances in BaU_2Se_5 are consistent with those found in U_3Se_5,[19] $RbAgUSe_3$,[40] and $CsAgUSe_3$.[40] All are typical for U^{4+} compounds. Owing to the actinide contraction,[41] the U–S distances in M = Sr, Pb, and Ba are shorter than the corresponding Th–S distances in the $BaTh_2S_5$ structure. Th–S distances (2.744(2)–3.025 Å) in the $BaTh_2S_5$ structure are in agreement with those observed in $Ba_2Cu_2ThS_5$ (2.743(1)–2.809(1) Å),[42] $KCuThS_3$ (2.7838(5)–2.7872(2) Å),[43] $K_2Cu_2ThS_4$ (2.781(3)–2.794(2) Å),[43] $K_3Cu_3Th_2S_7$ (2.75(2)–2.82(2) Å),[43] and Ba_2ThS_6 (2.889(1)–2.7759(3) Å).[9]

BaU_2Te_5. The crystal structure of BaU_2Te_5 differs from the one above. This compound crystallizes in the $(NH_4)Pb_2Br_5$[39] structure type with four formula units in space group D_{4h}^{18}–$I4/mcm$ of the tetragonal system (Table 1). The asymmetric unit contains one U atom, one Ba atom, and two Te atoms of site symmetries *m*.2*m*, 422, ..*m*, and 4/*m*.., respectively. A general projection of the structure is shown in Figure 5, and metrical

dx.doi.org/10.1021/ic501795w | *Inorg. Chem.* 2014, 53, 11626–11632

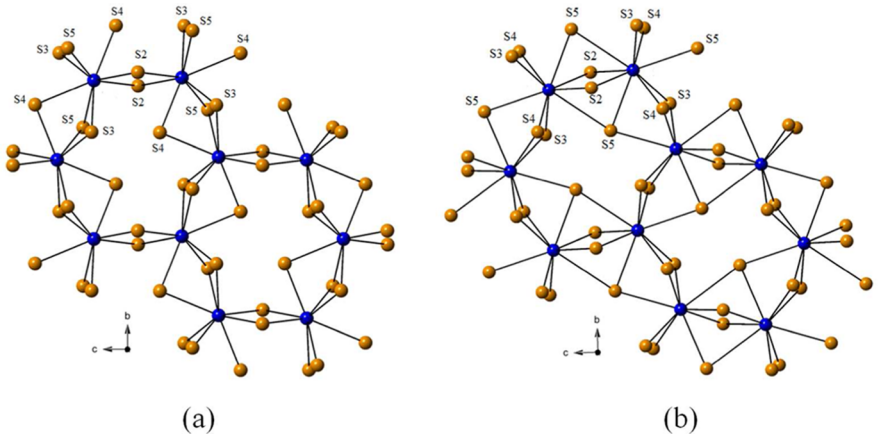

Figure 4. M/Q network viewed along the [100] direction in (a) PbU_2Se_5 and (b) $BaTh_2S_5$, SrU_2S_5, BaU_2Se_5, and BaU_2S_5.

Table 2. Selected Interatomic Lengths (Å)[a] in the MAn_2Q_5 Family[b]

compound	An1-Q	An2-Q	M-Q
SrU_2S_5	2.749(1)−2.978(1)	2.655(1)−2.882(1)	2.965(1)−3.589(1)
PbU_2S_5	2.765(2)−2.964(2)	2.663(2)−2.840(2)	2.786(2)−3.401(2)
BaU_2S_5[13]	2.731(1)−2.989(1)	2.683(1)−2.897(1)	3.066(1)−3.475(1)
$BaTh_2S_5$	2.833(2)−3.025(2)	2.744(2)−2.928(2)	3.077(2)−3.628(2)
BaU_2Se_5	2.858(1)−3.110(1)	2.807(1)−3.012(1)	3.190(1)−3.618(1)
PbU_2Se_5[17]	2.915(4)−3.105(3)	2.782(4)−2.960(3)	2.949(5)−3.503(4)
BaU_2Te_5	3.063(1) × 2		3.574(1) × 8
	3.219(1) × 4		3.641(1) × 2
	3.148(1) × 2		

[a]All distances have been rounded to facilitate comparisons. [b]The shortest U−U interactions in these structures are longer than 4.07 Å, except for the 3.6419(3) Å distance in BaU_2Te_5.

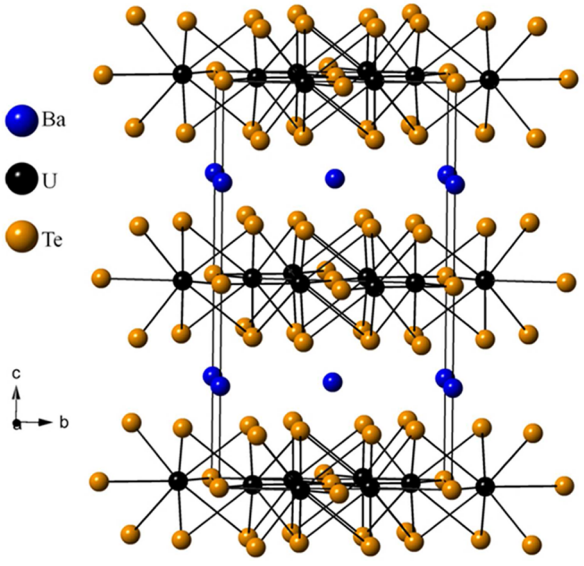

Figure 5. A general projection of the BaU_2Te_5 structure down the *a* axis.

data are given Table 2. In the BaU_2Te_5 structure, each U atom is coordinated to eight Te atoms to form a bicapped trigonal prism (Figure 6). Each U atom is connected to seven other U neighbors by Te atoms. The U atom shares a rectangular face composed of four Te1 atoms with its closest neighbor (U−U = 3.642 Å); it shares four Te1−Te1 edges with four U neighboring atoms (U−U = 4.451 Å); and it shares two corners via atom Te2 (U−U = 6.295 Å). The connections of

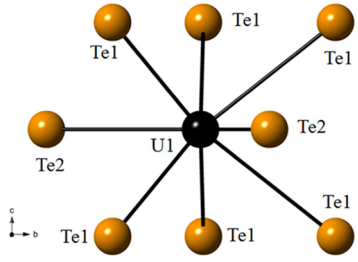

Figure 6. Local coordination environment of the U atoms in the crystal structure of BaU_2Te_5.

these polyhedra form infinite two-dimensional layers perpendicular to the *c* axis; these layers are separated by Ba atoms (Figure 7). Each Ba atom is connected to 10 Te atoms. The U−Te distances found in the structure of the BaU_2Te_5 may be compared with those in related compounds (Table 3) in which U also has a coordination number of eight.

Resistivity Studies. High-temperature-dependent resistivity data on single crystals of SrU_2S_5, BaU_2Se_5, and PbU_2S_5 along an arbitrary direction showed metallic behavior for all three (Figure 8). The metallic character measured experimentally is also in agreement with the electronic structure calculations. BaU_2Se_5 is the most resistive member in the series with a resistivity of 10 mΩ·cm at 298 K and 13 mΩ·cm at 700 K. SrU_2S_5 is the least resistive sample with a resistivity of 0.24 mΩ·cm at 298 K and 0.44 mΩ·cm at 700 K. The resistivity values of PbU_2S_5 are 3.3 and 6.7 mΩ·cm at 298 and 700 K, respectively.

DFT Calculations. The electronic structures of the four U compounds characterized in this study show remarkable

dx.doi.org/10.1021/ic501795w | *Inorg. Chem.* 2014, 53, 11626−11632

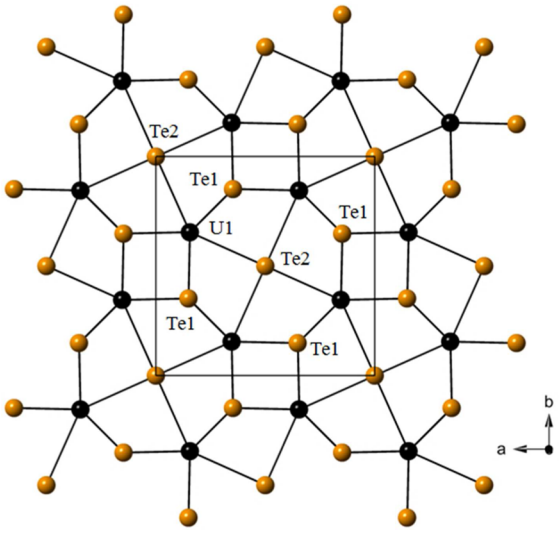

Figure 7. Two-dimensional layers in the BaU_2Te_5 structure.

Table 3. U−Te Interactions in Some Related Compounds[a]

compound	structure	U−Te distances (Å)	reference
BaU_2Te_5	layered	3.063(1)−3.219(1)	this work
UTe_2	3-dimensional	3.076(1)−3.201(1)	46
$CsZrUTe_5$	layered	3.096(1)−3.360(1)	47
$CsTiUTe_5$	layered	3.059(1)−3.262(1)	48
CsU_2Te_6	layered	3.089(1)−3.203(1)	49
$Cu_{0.78}U_2Te_6$	layered	3.100(1)−3.236(1)	50
$Tl_{0.56}UTe_3$	layered	3.093(2)−3.225(1)	51
$CsTiU_3Te_9$	3-dimensional	2.966(3)−3.276(3)	52

[a]The U atom is coordinated to eight Te atoms in all of these structures.

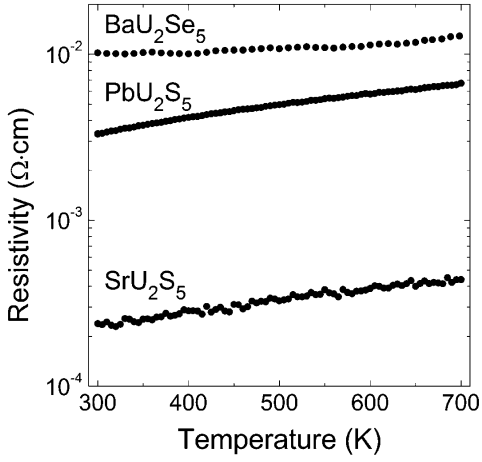

Figure 8. Variation of resistivity with temperature for SrU_2S_5, PbU_2S_5, and BaU_2Se_5.

similarities in their properties. The calculations suggest that all are ferromagnetic. In each, the density of states of one spin channel is finite at the Fermi level, whereas there is a gap in the density of states of the other spin channel; this is characteristic of a half-metal. In Figures 9 and 10, we present the calculated total (upper plot) and partial (lower plots) density of states for BaU_2Se_5 and BaU_2Te_5. The half-metallic nature of the compounds appears clearly from the total density of states, with a large value at the Fermi level (put at 0 eV) for the spin up, while it is zero for the spin down. From the partial density of states of the different U atoms, it is seen that the states at the Fermi level originate almost exclusively from U-f states, with a small contribution from Ba-d and S-p states. The finite magnetic moment on each U atom induces a small spin polarization on the other atoms, as seen by the unsymmetric partial density of states of the S and Ba species. BaU_2S_5 and PbU_2S_5 show a very similar distribution of states as a function of the energy. To illustrate the electronic structure of PbU_2S_5 in a different manner, we have calculated its band structure along some high-symmetry directions, as presented for each spin direction in Figure 11 (spin up) and in Figure 12 (spin down). Also, the character of the bands derived from U-f states appears as blue dots (the size of each dot being proportional to the importance of the U-f states for each band and for each calculated point along the path in the Brillouin zone). This highlight clearly illustrates that the states around the Fermi level are dominantly of f character for the spin up, whereas for the spin down there is a gap of approximately 2 eV, with the states immediately above the Fermi level being of U-f character.

Structure Type. Earlier, the question was addressed[44] of why some AB_2X_5 compounds crystallize in the monoclinic structure of the $(NH_4)Pb_2Cl_5$ type (now designated the PbU_2Se_5 type), whereas others crystallize in the tetragonal $(NH_4)Pb_2Br_5$ structure type. It was shown for the AB_2X_5 compounds (A = K, In, Tl; B = Sr, Sn, Pb; X = Cl, Br, I) that those with monoclinic structures could be separated from those with tetragonal structures by an empirical relationship involving the radii ratios A/X and B/X. The limitations of the use of radii ratios to predict complex ionic structure types are well-known and have been for almost 90 years,[45] so it is unfortunate, but not surprising, that a similar empirical approach fails to work for the BaU_2S_5, BaU_2Se_5, BaU_2Te_5 sequence in the present MAn_2Q_5 compounds.

CONCLUSIONS

Five ternary actinide chalcogenides, namely, SrU_2S_5, BaU_2Se_5, PbU_2S_5, $BaTh_2S_5$, and BaU_2Te_5 of the MAn_2Q_5 family, were obtained by solid-state reactions at temperatures ranging between 1123 and 1273 K. The sulfide and the selenide members are isostructural and crystallize in the PbU_2Se_5 structure type in space group C_{2h}^5−$P2_1/c$ of the monoclinic system. The three-dimensional structure comprises AnQ_8, AnQ_7, and MQ_8 or MQ_9 polyhedra. The AnQ_8 polyhedron is a bicapped trigonal prism; the AnQ_7 polyhedron is a distorted face-capped octahedron. Whether the structure is described as containing MQ_8 or MQ_9 polyhedra depends on the value of the monoclinic β angle. In contrast, the telluride member of this family, BaU_2Te_5, crystallizes in the $(NH_4)Pb_2Br_5$ structure type in space group D_{4h}^{18}−$I4/mcm$ of the tetragonal system. This layered structure comprises bicapped trigonal-prismatic UTe_8 polyhedra and $BaTe_{10}$ polyhedra. The formulas of these compounds can be charge balanced as $M^{2+}(An^{4+})_2(Q^{2-})_5$ because there is no Q−Q bonding. Resistivity studies on single crystals of SrU_2S_5, BaU_2Se_5, and PbU_2S_5 show metallic behavior with resistivities of 0.24, 10, and 3.3 mΩ·cm, respectively, at 298 K. Calculations using spin-polarized density functional theory in the generalized gradient approximation show that the electronic structures of the four U compounds are remarkably similar. In each compound, the density of states of one spin channel is found to be finite at the Fermi level, whereas there is a gap of approximately 2 eV in the density of states of the other spin channel; this is characteristic of a half-metal.

dx.doi.org/10.1021/ic501795w | Inorg. Chem. 2014, 53, 11626−11632

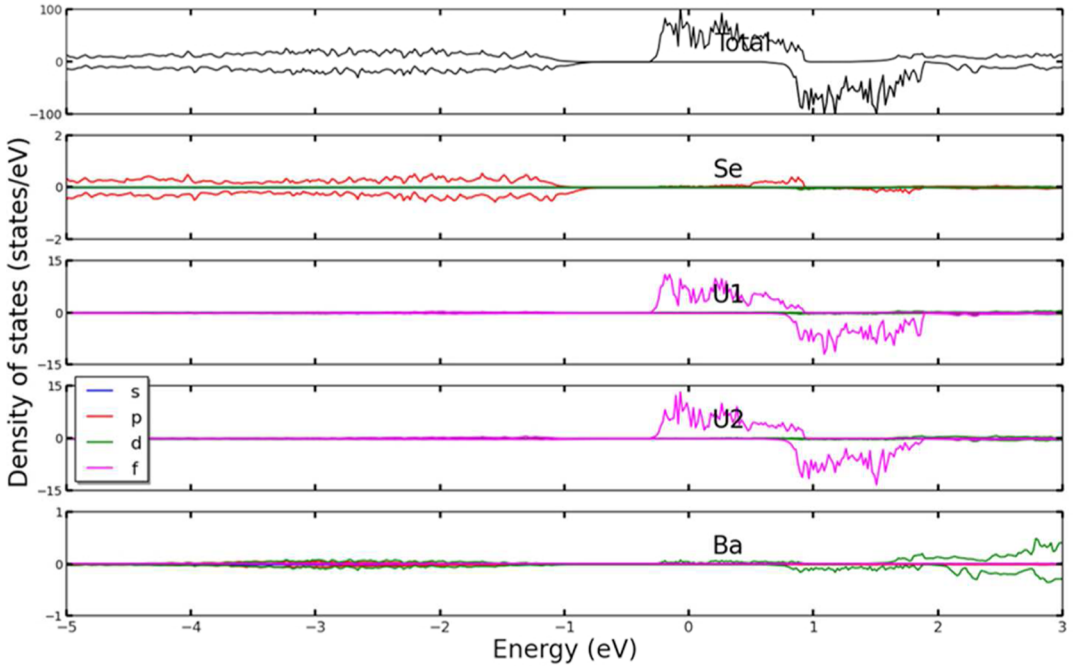

Figure 9. Calculated total (upper plot) and partial (lower plots) density of states for BaU_2Se_5.

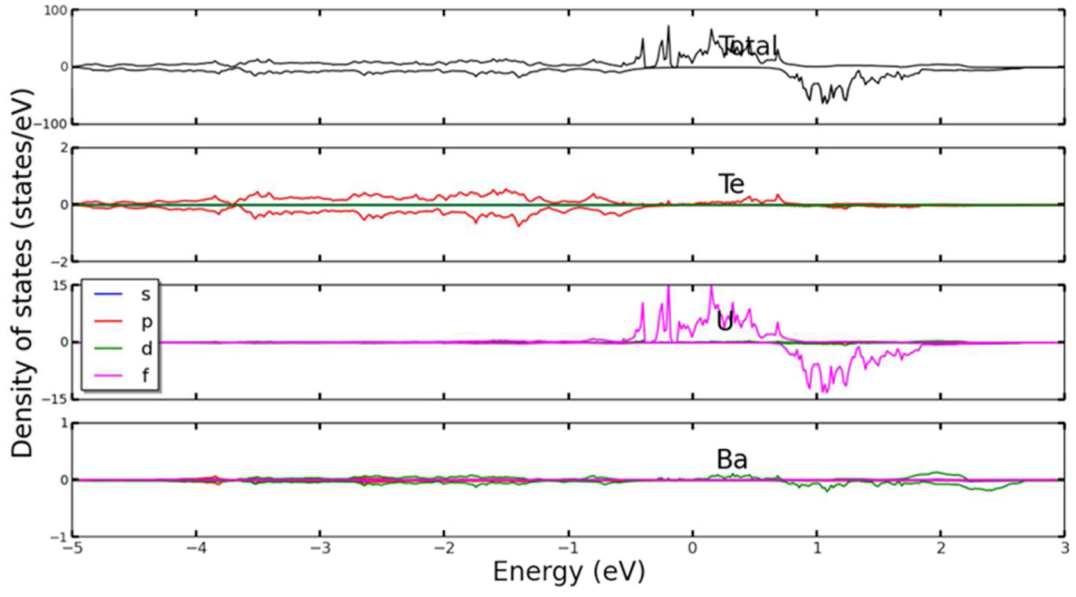

Figure 10. Calculated total (upper plot) and partial (lower plots) density of states for BaU_2Te_5.

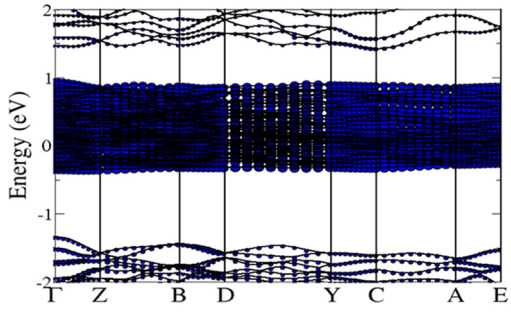

Figure 11. Upper plot: band structure of PbU_2S_5 for the spin-up; the character of the bands corresponding to U-f states appears as blue dots. The Fermi level is at 0 eV.

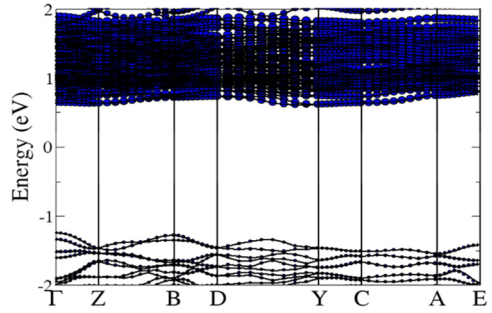

Figure 12. Lower plot: band structure of PbU_2S_5 for the spin-down; the character of the bands corresponding to U-f states appears as blue dots. The Fermi level is at 0 eV.

dx.doi.org/10.1021/ic501795w | *Inorg. Chem.* 2014, 53, 11626−11632

■ ASSOCIATED CONTENT

Supporting Information

Crystallographic file in cif format for SrU_2S_5, BaU_2Se_5, PbU_2S_5, $BaTh_2S_5$, and BaU_2Te_5. This material is available free of charge via the Internet at http://pubs.acs.org.

■ AUTHOR INFORMATION

Corresponding Author

*E-mail: ibers@chem.northwestern.edu (J.A.I.).

Notes

The authors declare no competing financial interest.

■ ACKNOWLEDGMENTS

Use was made of the IMSERC X-ray Facility at Northwestern University, supported by the International Institute of Nanotechnology (IIN). S.L. acknowledges HPC resources from GENCI-CCRT/CINES (Grant x2014-085106).

■ REFERENCES

(1) Riley, B. J.; Chun, J.; Um, W.; Lepry, W. C.; Matyas, J.; Olszta, M. J.; Li, X.; Polychronopoulou, K.; Kanatzidis, M. G. *Environ. Sci. Technol.* **2013**, *47*, 7540−7547.

(2) Manos, M. J.; Kanatzidis, M. G. *J. Am. Chem. Soc.* **2009**, *131*, 6599−6607.

(3) Manos, M. J.; Kanatzidis, M. G. *Chem.—Eur. J.* **2009**, *15*, 4779−4784.

(4) Mertz, J.; Fard, Z. H.; Malliakas, C. M.; Manos, M. J.; Kanatzidis, M. G. *Chem. Mater.* **2013**, *25*, 2116−2127.

(5) Bugaris, D. E.; Ibers, J. A. *Dalton Trans.* **2010**, *39*, 5949−5964.

(6) Narducci, A. A.; Ibers, J. A. *Chem. Mater.* **1998**, *10*, 2811−2823.

(7) Manos, E.; Kanatzidis, M. G.; Ibers, J. A. In *The Chemistry of the Actinide and Transactinide Elements*, 4th ed.; Morss, L. R., Edelstein, N. M., Fuger, J., Eds.; Springer: Dordrecht, The Netherlands, 2010; Vol. *6*, pp 4005−4078.

(8) Koscielski, L. A.; Ibers, J. A. *Z. Anorg. Allg. Chem.* **2012**, *638*, 2585−2593.

(9) Mesbah, A.; Ringe, E.; Lebègue, S.; Van Duyne, R. P.; Ibers, J. A. *Inorg. Chem.* **2012**, *51*, 13390−13395.

(10) Narducci, A. A.; Ibers, J. A. *Inorg. Chem.* **1998**, *37*, 3798−3801.

(11) Brochu, R.; Padiou, J.; Grandjean, D. *C. R. Seances Acad. Sci., Ser. C* **1970**, *271*, 642−643.

(12) Lelieveld, R.; IJdo, D. J. W. *Acta Crystallogr., Sect. B: Struct. Crystallogr. Cryst. Chem.* **1980**, *36*, 2223−2226.

(13) Mesbah, A.; Ibers, J. A. *J. Solid State Chem.* **2013**, *199*, 253−257.

(14) Komac, M.; Golic, L.; Kolar, D.; Brcic, B. S. *J. Less-Common Met.* **1971**, *24*, 121−128.

(15) Brochu, R.; Padiou, J.; Prigent, J. *C. R. Acad. Sci. Paris* **1970**, *270*, 809−810.

(16) Brochu, R.; Padiou, J.; Prigent, J. *C. R. Seances Acad. Sci., Ser. C* **1972**, *274*, 959−961.

(17) Potel, M.; Brochu, R.; Padiou, J. *Mater. Res. Bull.* **1975**, *10*, 205−208.

(18) Potel, M.; Brochu, R.; Padiou, J.; Grandjean, D. *C. R. Seances Acad. Sci., Ser. C* **1972**, *275*, 1419−1421.

(19) Moseley, P. T.; Brown, D.; Whittaker, B. *Acta Crystallogr.* **1972**, *B28*, 1816−1821.

(20) Bugaris, D. E.; Ibers, J. A. *J. Solid State Chem.* **2008**, *181*, 3189−3193.

(21) Haneveld, A. J. K.; Jellinek, F. *J. Less-Common Met.* **1969**, *18*, 123−129.

(22) Cordier, G.; Schwidetzky, C.; Schaefer, H. *Rev. Chim. Miner.* **1982**, *19*, 179−186.

(23) Jin, G. B.; Raw, A. D.; Skanthakumar, S.; Haire, R. G.; Soderholm, L.; Ibers, J. A. *J. Solid State Chem.* **2010**, *183*, 547−550.

(24) Koscielski, L. A.; Ringe, E.; Van Duyne, R. P.; Ellis, D. E.; Ibers, J. A. *Inorg. Chem.* **2012**, *51*, 8112−8118.

(25) *Bruker APEX2 Version 2009.5-1: Data Collection and Processing Software*; Bruker Analytical X-Ray Instruments, Inc.: Madison, WI, 2009.

(26) Sheldrick, G. M. *SADABS*; Department of Structural Chemistry, University of Göttingen: Göttingen, Germany, 2008.

(27) Sheldrick, G. M. *Acta Crystallogr., Sect. A: Found. Crystallogr.* **2008**, *64*, 112−122.

(28) Gelato, L. M.; Parthé, E. *J. Appl. Crystallogr.* **1987**, *20*, 139−143.

(29) Spek, A. L. *PLATON: A Multipurpose Crystallographic Tool*; Utrecht University: Utrecht, The Netherlands, 2014.

(30) Kresse, G.; Forthmüller, J. *Comput. Mater. Sci.* **1996**, *6*, 15−50.

(31) Kresse, G.; Joubert, D. *Phys. Rev. B* **1999**, *59*, 1758−1775.

(32) Blöchl, P. E. *Phys. Rev. B* **1994**, *50*, 17953−17979.

(33) Hohenberg, P.; Kohn, W. *Phys. Rev.* **1964**, *136*, 864−871.

(34) Kohn, W.; Sham, L. J. *Phys. Rev.* **1965**, *140*, 1133−1138.

(35) Perdew, J. P. In *Electronic Structure of Solids*; Ziesche, P., Eschrig, H., Eds.; Akademie Verlag: Berlin, 1991; pp 11−20.

(36) Ward, M. D.; Ibers, J. A. *Z. Anorg. Allg. Chem.* **2014**, *640*, 1585−1588.

(37) Troc, R.; Zolnierek, Z. *J. Phys. (Paris)* **1979**, *C4*, 79−81.

(38) Amoretti, G.; Blaise, A.; Collard, J. M.; Hall, R. O. A.; Mortimer, M. J.; Troc, R. *J. Magn. Magn. Mater.* **1984**, *46*, 57−67.

(39) Powell, H. M.; Tasker, H. S. *J. Chem. Soc.* **1937**, 119−123.

(40) Yao, J.; Wells, D. M.; Chan, G. H.; Zeng, H.-Y.; Ellis, D. E.; Van Duyne, R. P.; Ibers, J. A. *Inorg. Chem.* **2008**, *47*, 6873−6879.

(41) Shannon, R. D. *Acta Crystallogr., Sect. A: Cryst. Phys., Diffr., Theor. Gen. Crystallogr.* **1976**, *32*, 751−767.

(42) Mesbah, A.; Lebegue, S.; Klingsporn, J. M.; Stojko, W.; Van Duyne, R. P.; Ibers, J. A. *J. Solid State Chem.* **2013**, *200*, 349−353.

(43) Selby, H. D.; Chan, B. C.; Hess, R. F.; Abney, K. D.; Dorhout, P. K. *Inorg. Chem.* **2005**, *44*, 6463−6469.

(44) Beck, H. P.; Clicqué, G.; Nau, H. *Z. Anorg. Allg. Chem.* **1986**, *536*, 35−44.

(45) Pauling, L. *J. Am. Chem. Soc.* **1927**, *49*, 765−790.

(46) Beck, H. P.; Dausch, W. *Z. Naturforsch., B: J. Chem. Sci.* **1988**, *43*, 1547−1550.

(47) Kim, J.-Y.; Gray, D. L.; Ibers, J. A. *Acta Crystallogr., Sect. E: Struct. Rep. Online* **2006**, *E62*, i124−i125.

(48) Cody, J. A.; Ibers, J. A. *Inorg. Chem.* **1995**, *34*, 3165−3172.

(49) Mesbah, A.; Ibers, J. A. *Acta Crystallogr., Sect. E: Struct. Rep. Online* **2012**, *68*, i76.

(50) Huang, F. Q.; Ibers, J. A. *J. Solid State Chem.* **2001**, *159*, 186−190.

(51) Tougait, O.; Daoudi, A.; Potel, M.; Noël, H. *Mater. Res. Bull.* **1997**, *32*, 1239−1245.

(52) Ward, M. D.; Mesbah, A.; Lee, M.; Malliakas, C. D.; Choi, E. S.; Ibers, J. A. *Inorg. Chem.* **2014**, *53*, 7909−7915.